Local structure and medium-range ordering in relaxor ferroelectric Pb (Zn 1 3 Nb 2 3) O 3 studied using neutron pair distribution function analysis

I.-K. Jeong and J. K. Lee

Citation: Applied Physics Letters **88**, 262905 (2006); doi: 10.1063/1.2217162
View online: http://dx.doi.org/10.1063/1.2217162
View Table of Contents: http://scitation.aip.org/content/aip/journal/apl/88/26?ver=pdfcov
Published by the AIP Publishing

Articles you may be interested in

Dielectric and piezoelectric properties of (1 x) (Bi 1 y Li y) (Sc 1 y Sb y) O 3 – x Pb Ti O 3 high-temperature relaxor ferroelectric ceramics
Appl. Phys. Lett. **93**, 022904 (2008); 10.1063/1.2960361

Uniaxial-stress induced phase transitions in [001] C -poled 0.955 Pb (Zn 1 3 Nb 2 3) O 3 – 0.045 Pb Ti O 3
Appl. Phys. Lett. **90**, 152907 (2007); 10.1063/1.2721856

Growth and electrical properties of large size Pb (In 1 2 Nb 1 2) O 3 – Pb (Mg 1 3 Nb 2 3) O 3 – Pb Ti O 3 crystals prepared by the vertical Bridgman technique
Appl. Phys. Lett. **90**, 032901 (2007); 10.1063/1.2431706

High temperature dc field poling effects on the structural phase transformations of (1 x) Pb (Mg 1 3 Nb 2 3) O 3 – x Pb Ti O 3 single crystal with morphotropic phase boundary composition
J. Appl. Phys. **100**, 064107 (2006); 10.1063/1.2337103

Raman spectroscopy study of ferroelectric modes in [001]-oriented 0.67 Pb (Mg 1 3 Nb 2 3) O 3 – 0.33 PbTiO 3 single crystals
Appl. Phys. Lett. **86**, 252903 (2005); 10.1063/1.1948514

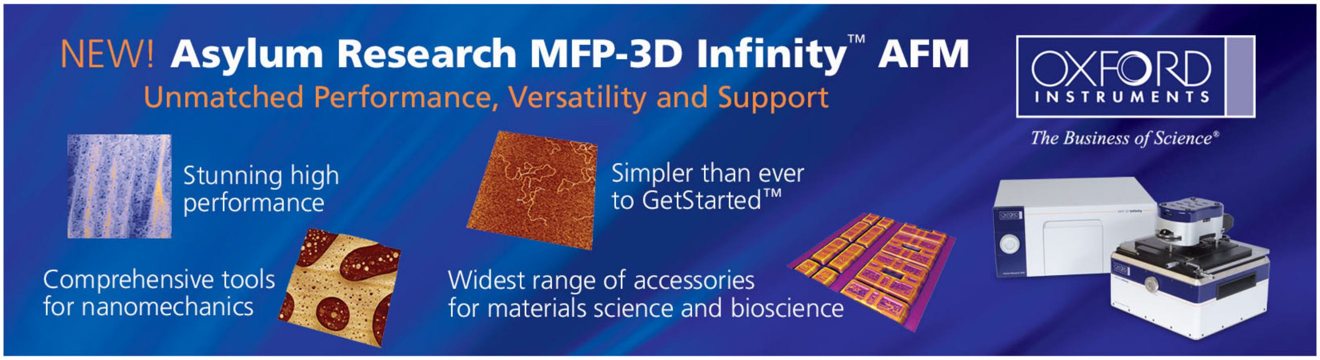
NEW! Asylum Research MFP-3D Infinity™ AFM
Unmatched Performance, Versatility and Support
Stunning high performance
Simpler than ever to GetStarted™
Comprehensive tools for nanomechanics
Widest range of accessories for materials science and bioscience
OXFORD INSTRUMENTS
The Business of Science®

This article is copyrighted as indicated in the article. Reuse of AIP content is subject to the terms at: http://scitation.aip.org/termsconditions. Downloaded to IP: 130.49.166.18 On: Fri, 02 May 2014 18:11:21

APPLIED PHYSICS LETTERS **88**, 262905 (2006)

Local structure and medium-range ordering in relaxor ferroelectric $Pb(Zn_{1/3}Nb_{2/3})O_3$ studied using neutron pair distribution function analysis

I.-K. Jeong[a] and J. K. Lee
Los Alamos National Laboratory, Los Alamos, New Mexico 87545

(Received 6 January 2006; accepted 12 May 2006; published online 28 June 2006)

We studied an evolution of local structure and medium-range ordering in relaxor ferroelectric $Pb(Zn_{1/3}Nb_{2/3})O_3$ (PZN) from 550 to 15 K using neutron pair distribution function analysis. We show that the local structure of PZN is distorted at all temperatures studied. With decreasing temperature, a medium-range ordering of local polarizations develops with no global rhombohedral phase transition below T_M. Instead, the crystal structure can be described as a mixture of polar nanoregions in a disordered lattice, similar to the case of $Pb(Mg_{1/3}Nb_{2/3})O_3$. © *2006 American Institute of Physics*. [DOI: 10.1063/1.2217162]

Relaxor ferroelectrics hold great scientific interests as well as potential for industrial applications due to their high, relatively temperature-independent, permittivities. Dielectric properties of relaxor ferroelectrics[1] such as $Pb(Mg_{1/3}Nb_{2/3})O_3$ (PMN) and $Pb(Zn_{1/3}Nb_{2/3})O_3$ (PZN) are fundamentally different from those of normal ferroelectrics and are similar to spin glasses.[2] It is believed that characteristics of relaxor ferroelectrics result from structural and chemical disorders and a formation of polar nanoregions (PNRs) at temperatures well above the maximum temperature of permittivities (T_M).[3,4]

In a prototypical relaxor ferroelectric PMN, the average crystal structure remains cubic over the temperature range from 1000 to 5 K. Nevertheless, many experimental results including refractive index,[5] electrostriction,[6] and elastic diffuse scattering[7] measurements suggest a presence of local polarizations and a spatial correlation (ξ) of atomic displacements at temperatures a few hundred degrees above T_M. In a similar relaxor ferroelectric PZN, the crystal structure looks more complex. Below T_M ($\sim$410 K), Bragg peaks gradually split over the temperature range from $T=385$ to 325 K, indicating a diffusive structural phase transition to rhombohedral phase.[8] Furthermore, Xu *et al.*[9] reported intriguing results on the crystal structure of single crystal PZN. At 300 K, Xu *et al.* found that the bulk structure probed using highly penetrating 67 keV x ray is nearly cubic ("X phase") and is completely different from the rhombohedral structure of an outer layer of about 10–50 μm. Based on their findings, Xu *et al.* proposed that PZN does not undergo rhombohedral phase transition below T_M but is best described by PNRs spread in a nearly cubic lattice.[9] However, the existence of the X phase is still controversial.[10]

In this letter, we studied the complicated crystal structure of PZN using neutron pair distribution function (PDF) analysis. We report temperature evolution of local (<5 Å) and medium-range ($\sim$5–20 Å) structure from 550 to 15 K and discuss the issue of the global rhombohedral phase transition below T_M. The PDF technique has long been used to characterize structures of glasses, liquids, and amorphous materials[11] and recently found its application to study local structures of disordered crystalline materials[12,13] and correlated atomic motions of atom pairs.[14] From an atomic structural point of view, local polarizations can be considered as a result of symmetry breaking local atomic displacements and PNRs due to a medium-range ordering of local atomic displacements. Therefore, we expect that PDF studies on PZN will provide a valuable structural information in understanding the complex phase transition and the relaxor behavior of PZN.

The experiments were performed on NPDF instrument at the Los Alamos Neutron Science Center (LANSCE). Powder diffraction data were corrected for background, absorption, and multiple scattering, and normalized using a vanadium spectrum to obtain total scattering (diffuse scattering +Bragg peaks) structure function $S(Q)$, using the PDFGETN program.[15] The PDF $G(r)$ is obtained from $S(Q)$ via the sine Fourier transform shown in Eq. (1),

$$G(r) = 4\pi r[\rho(r) - \rho_0] = \frac{2}{\pi}\int_0^{Q_{\max}} Q[S(Q) - 1]\sin QrdQ, \quad (1)$$

and measures the probability of finding an atom at a distance r from another atom. Here, Q is a wave vector and $\rho(r)$ and ρ_0 are the atomic pair number density and average number density, respectively.

Figures 1(a) and 1(b) show reduced structure function $Q[S(Q)-1]$ and the corresponding experimental PDF of PZN at 15 K, respectively. Also shown in the inset of Fig. 1(a) is a cubic perovskite structure of PZN. In Fig. 1(b), we notice a splitting of Zn/Nb–O bond into two peaks and Pb–O bond into three peaks due to local atomic displacements of Zn/Nb and Pb ions in O_6 and O_{12} cages [see the inset of Fig. 1(a)], respectively. In addition, relative displacements of Pb from Zn/Nb ions induce a splitting of Zn/Nb–Pb peak.

On the directions of local atomic displacements in PZN and PMN, a short-range correlation along the $\langle 110\rangle$ direction[7,16,17] and a tetragonal [001]-[18] and [111]-type displacements[19–21] have been proposed from diffuse scattering, x-ray absorption fine structure analysis, and ^{207}Pb nuclear-magnetic-resonance measurements. These competing results are due to complexity of the local structures resulted from strong chemical and structural disorders. We modeled the local structure of PZN using PDF at 15 K. For Pb dis-

---

[a] Author to whom correspondence should be addressed; electronic mail: jeong@lanl.gov

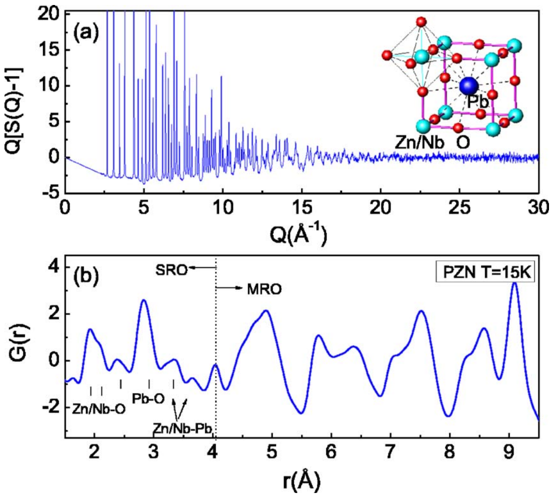

FIG. 1. (Color online) (a) Reduced structure function $Q[S(Q)-1]$ of PZN at 15 K. The inset shows a cubic perovskite structure of PZN. (b) Corresponding experimental PDF {sine Fourier transform of $Q[S(Q)-1]$}. PDF spectrum provides structural information on short-range ordering (SRO) below $r\sim 4$ Å and medium-range ordering above $r\sim 4$ Å, respectively. Zn/Nb–O peak, Pb–O peak, and Zn/Nb–Pb peaks are split due to local displacements of Zn/Nb and Pb ions. The tick marks represent Zn/Nb–O and Pb–O pair distances assuming [111] local displacements of Zn/Nb and Pb ions relative to O_6 and O_{12} cages, respectively.

placements, we found that [111]-type displacement which splits the Pb–O bond into three peaks with 3:6:3 amplitude ratio, describes the splitting of experimental Pb–O PDF peak much better than either [110]- or [001]-type displacements. For Zn/Nb displacements, [001]-type displacement is ruled out because the splitting of Zn/Nb–O bond into three peaks with the 1:4:1 amplitude ratio does not match with the experimental result. However, between [110] and [111] displacements, it was not easy to differentiate one from the other due to too many factors affecting the Zn/Nb–O PDF peak shape such as non-negligible Zn displacement.[22] For simplicity, we assumed [111]- type displacements for all ions in model PDF calculations shown later. The tick marks in Fig. 1(b) represent Zn/Nb–O and Pb–O pair distances assuming [111] local displacements of Zn/Nb and Pb ions relative to O_6 and O_{12} cages, respectively.

Figure 2(a) shows a temperature evolution of local structure ($r\leq 4$ Å) of PZN from 550 to 15 K. For clarity, the spectra are shifted from each other. Here we observe a few interesting features. First, at 550 K (above T_M) Zn/Nb–O peak shows a weak shoulder on high r side, indicating a local Zn/Nb displacement. With decreasing temperature, this shoulder becomes more clearly resolved without much change in the peak shape. Thus, from this temperature dependence, we can speculate that local atomic displacement of Zn/Nb does not change much from 550 to15 K and the gradual resolution of Zn/Nb–O bonds is mostly due to decreasing thermal motions. Second, we notice a well defined peak around $r=2.4$ Å at all temperatures. Referring to the inset in Fig. 1(a), we can assign this peak to a short Pb–O bond created by a local Pb displacement in O_{12} cage. Density function theory calculations[22] show that Pb ions in many Pb-containing perovskite displace about 0.4 Å from the center of oxygen cage due to lone pair electrons in Pb^{2+} that strongly hybridize with O $2p$ states.[23] Finally, the peak position at $r\sim 4.04$ Å which measures the lattice parameter is more or less temperature independent in spite of strong local distortions.

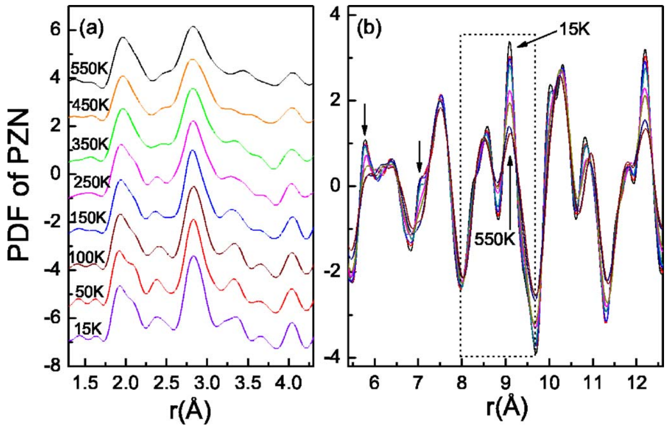

FIG. 2. (Color online) (a) Temperature evolution of local structure ($r\leq 4$ Å) of PZN from $T=550$ to 15 K. For clarity, PDF spectra are shifted from each other. (b) PDF spectra of PZN from $T=550$ to 15 K in the medium range of 5 Å$<r<$13 Å. The arrows indicate peaks displaying an anomalous temperature dependence.

We now address a medium-range ordering of local atomic displacements. Figure 2(b) shows PDF spectra of PZN from 550 to 15 K in the r range of 5 Å$<r<$13 Å. Here we notice that PDF peaks at $r\sim 5.8$ Å and $r\sim 7.05$ Å grow significantly with decreasing temperature. In addition, the PDF peaks in the doublet in the range of 8.0 Å$<r<$9.85 Å show very distinct temperature dependence from each other. In similar relaxor ferroelectric PMN, the peaks in the doublet showed almost same behavior as those in PZN.[24] Therefore, we expect that both PZN and PMN have the same origin for the anomalous temperature evolution of PDF peaks in the medium range, namely, the formation of polar nanoregions.

To examine the origin of the structural features in the experimental PDF spectra, we calculated three model PDFs using simple crystal structures. First, we tested whether the structure of PZN at 15 K can be described by a well ordered rhombohedral structure $R3m$ (single unit cell repeating in three dimensions). In this model, Pb and Zn/Nb ions are shifted along the [111] direction relative to oxygen ions and the rhombohedral angle is $\alpha=89.9°$. We used thermal parameters, $B_{Pb}=0.3363$, $B_{Zn/Nb}=0.1570$, and $B_O=0.2465$ Å^2 found at 15 K, in well ordered perovskite compounds such as $PbTiO_3$ and $BaTiO_3$ (Ref. 25) because thermal parameters are not easily separated from highly disordered atomic displacements in the Rietveld refinement.[26] Figure 3(a) shows that peak positions in the model PDF match quite well with those in experimental PDF. However, we notice that peaks in the model PDF are much sharper than peaks in the experimental PDF. This discrepancy indicates that the real crystal structure of PZN is highly disordered[13] and cannot be described by a single phase rhombohedral structure.

Next, we took an opposite approach. We obtained a disordered structure (10×10×10 unit cells) via a reverse Monte Carlo (RMC) fit to the experimental PDF at 550 K, using the DISCUS program.[27] In the RMC fit, the thermal parameters were fixed to the value found in well ordered perovskite compounds at 550 K.[25] Since the temperature of 550 K is much lower than the Burn temperature of PZN ($T_d\sim 750$ K), we expect to have some degrees of spatial correlation between atomic displacements at this temperature. After we obtained the model structure, we calculated a model

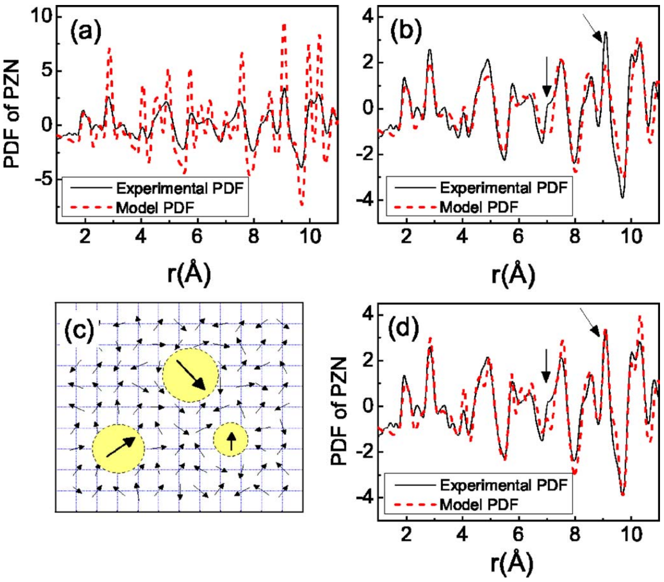

FIG. 3. (Color online) Comparison of experimental PDF (solid line) with model PDFs (dotted line) at 15 K. (a) Model PDF G_R is calculated using a well ordered rhombohedral crystal structure ($R3m$, $\alpha=89.9°$). (b) Model PDF G_D is calculated at 15 K using atomic positions obtained from a RMC fit to the PDF at 550 K and thermal parameters at 15 K. See text for details. (c) Schematic "two-phase (TP)" model structure. Medium-range ordered rhombohedral PNRs (circles) are dispersed on a disordered host structure (small arrows). The arrows represent local polarizations. (d) "Two-phase (TP)" model PDF, G_{TP} is calculated by $G_{TP}=0.8G_D+0.2G_R$.

PDF using thermal parameters at 15 K. In Fig. 3(b) we notice that the overall agreement between the model PDF and the experimental PDF has improved significantly. The agreement, however, is not quite good for experimental PDF peaks whose intensities are sensitive to the medium-range ordering as the arrows indicate.

As a third model, we assumed that well ordered rhombohedral regions (PNRs) develop on a highly disordered structure as shown in the schematic diagram of Fig. 3(c). To introduce the contributions of the well ordered rhombohedral regions to PDF intensities, we simply added model PDFs shown in Figs. 3(a) and 3(b) with a ratio. In Fig. 3(d) the two-phase model PDF G_{TP} is obtained by $G_{TP}=0.8G_D+0.2G_R$. This simple model PDF G_{TP} now captures most of missing features in model (b) as the arrows indicate.

Therefore, our simple model comparisons with experimental PDF suggest that the crystal structure of PZN at 15 K is better described by a mixed structure in which medium-range ordered, rhombohedral PNRs develop on a disordered structure. In PZN, these PNRs are simply larger ($\xi\sim150$ Å at 300 K)[28] than those in PMN ($\xi\sim20$ Å at 300 K) so they are visible in powder diffraction measurements as a split of Bragg peaks. Besides this difference, we propose that PZN and PMN have same ground state, i.e., mixed state of disordered cubic phase and rhombohedrally ordered PNRs, thus have the same mechanism for the relaxor behaviors.

The authors thank Th. Proffen for help with data collection. One of the authors (J.K.L.) is grateful to Professor K. S. Hong for providing PZN powder sample. The work at Los Alamos was carried out under the auspices of the U.S. DOE/Office of Science. The data were collected at the NPDF beamline at LANSCE, Los Alamos which is supported by the U.S. Department of Energy.

[1] G. A. Smolenskii and A. I. Agranovskaya, Sov. Phys. Solid State **1**, 1429 (1959).
[2] K. Binder and A. P. Young, Rev. Mod. Phys. **58**, 801 (1986).
[3] L. E. Cross, Ferroelectrics **76**, 241 (1987).
[4] G. A. Samara, J. Phys.: Condens. Matter **15**, R367 (2003).
[5] G. Burns and F. H. Dacol, Solid State Commun. **48**, 853 (1983).
[6] J. Zhao, A. E. Glazounov, Q. M. Zhang, and B. Toby, Appl. Phys. Lett. **72**, 1048 (1998).
[7] G. Xu, G. Shirane, J. R. D. Copley, and P. M. Gehring, Phys. Rev. B **69**, 064112 (2004).
[8] A. Lebon, H. Dammak, G. Calvarin, and I. O. Ahmedou, J. Phys.: Condens. Matter **14**, 7035 (2002).
[9] G. Xu, Z. Zhong, Y. Bing, Z.-G. Ye, C. Stock, and G. Shirane, Phys. Rev. B **67**, 104102 (2003).
[10] E. H. Kisi and J. S. Forrester, J. Phys.: Condens. Matter **17**, L381 (2005).
[11] Y. Waseda, *The Structure of Non-crystalline Materials* (McGraw-Hill, New York, 1980).
[12] V. Petkov, I.-K. Jeong, J. S. Chung, M. F. Thorpe, S. Kycia, and S. J. L. Billinge, Phys. Rev. Lett. **83**, 4089 (1999).
[13] T. Egami and S. J. L. Billinge, *Underneath the Bragg Peaks: Structural Analysis of Complex Materials* (Pergamon, Oxford, 2003).
[14] I.-K. Jeong, Th. Proffen, F. Mohiuddin-Jacobs, and S. J. L. Billinge, J. Phys. Chem. A **103**, 921 (1999).
[15] Th. Proffen and S. J. L. Billinge, J. Appl. Crystallogr. **32**, 572 (1999).
[16] H. You and Q. M. Zhang, Phys. Rev. Lett. **79**, 3950 (1997).
[17] T. R. Welberry, M. J. Gutmann, H. Woo, D. J. Goossens, G. Xu, C. Stock, W. Chen, and Z.-G. Ye, J. Appl. Crystallogr. **38**, 639 (2005).
[18] S. Vakhrushev, A. Ivanov, and J. Kulda, Phys. Chem. Chem. Phys. **7**, 2340 (2005).
[19] N. de Mathan, E. Husson, G. Calvarin, J. R. Gavarri, A. W. Hewat, and A. Morell, J. Phys.: Condens. Matter **3**, 8159 (1991).
[20] E. Prouzet, E. Husson, N. de Mathan, and A. Morell, J. Phys.: Condens. Matter **5**, 4489 (1993).
[21] R. Blinc, V. V. Laguta, and B. Zalar, Phys. Rev. Lett. **91**, 247601 (2003).
[22] I. Grinberg and A. M. Rappe, Phys. Rev. B **70**, 220101 (2004).
[23] R. E. Cohen, Nature (London) **358**, 136 (1992).
[24] I.-K. Jeong, T. W. Darling, J. K. Lee, T. Proffen, R. H. Heffner, J. S. Park, K. S. Hong, W. Dmowski, and T. Egami, Phys. Rev. Lett. **94**, 147602 (2005).
[25] P. Bonneau, P. Garnier, G. Calvarin, E. Husson, J. R. Cavarri, A. W. Hewat, and A. Morrel, J. Solid State Chem. **91**, 350 (1991).
[26] H. B. Bürgi, Annu. Rev. Phys. Chem. **51**, 275 (2000).
[27] Th. Proffen, and R. Neder, J. Appl. Crystallogr. **30**, 171 (1997).
[28] D. La-Orauttapong, J. Toulouse, J. L. Robertson, and Z.-G. Ye, Phys. Rev. B **64**, 212101 (2001).